Integrative and Comparative Biology Advance Access published October 9, 2014

Integrative and Comparative Biology

Integrative and Comparative Biology, pp. 1–10
doi:10.1093/icb/icu114

Society for Integrative and Comparative Biology

SYMPOSIUM

Scaling of the Spring in the Leg during Bouncing Gaits of Mammals

David V. Lee,[1,*] Michael R. Isaacs,* Trevor E. Higgins,[†] Andrew A. Biewener[†] and Craig P. McGowan[‡]

*School of Life Sciences, University of Nevada Las Vegas, Las Vegas, NV 89154, USA; [†]Concord Field Station, Harvard University, Bedford, MA 01730, USA; [‡]Department of Biological Sciences, University of Idaho, Moscow, ID 83844, USA

From the symposium "Terrestrial Locomotion: Where Do We Stand, Where Are We Going?" presented at the annual meeting of the Society for Integrative and Comparative Biology, January 3–7, 2014 at Austin, Texas.

[1]E-mail: david.lee@unlv.edu

Synopsis Trotting, bipedal running, and especially hopping have long been considered the principal bouncing gaits of legged animals. We use the radial-leg spring constant k_{rad} to quantify the stiffness of the physical leg during bouncing gaits. The radial-leg is modeled as an extensible strut between the hip and the ground and k_{rad} is determined from the force and deflection of this strut in each instance of stance. A Hookean spring is modeled in-series with a linear actuator and the stiffness of this spring k_{rad} is determined by minimizing the work of the actuator while reproducing the measured force-deflection dynamics of an individual leg during trotting or running, and of the paired legs during hopping. Prior studies have estimated leg stiffness using k_{leg}, a metric that imagines a virtual-leg connected to the center of mass. While k_{leg} has been applied extensively in human and comparative biomechanics, we show that k_{rad} more accurately models the spring in the leg when actuation is allowed, as is the case in biological and robotic systems. Our allometric analysis of k_{rad} in the kangaroo rat, tammar wallaby, dog, goat, and human during hopping, trotting, or running show that k_{rad} scales as body mass to the two-third power, which is consistent with the predictions of dynamic similarity and with the scaling of k_{leg}. Hence, two-third scaling of locomotor spring constants among mammals is supported by both the radial-leg and virtual-leg models, yet the scaling of k_{rad} emerges from work-minimization in the radial-leg model instead of being a defacto result of the ratio of force to length used to compute k_{leg}. Another key distinction between the virtual-leg and radial-leg is that k_{rad} is substantially greater than k_{leg}, as indicated by a 30–37% greater scaling coefficient for k_{rad}. We also show that the legs of goats are on average twice as stiff as those of dogs of the same mass and that goats increase the stiffness of their legs, in part, by more nearly aligning their distal limb-joints with the ground reaction force vector. This study is the first allometric analysis of leg spring constants in two decades. By means of an independent model, our findings reinforce the two-third scaling of spring constants with body mass, while showing that springs in-series with actuators are stiffer than those predicted by energy-conservative models of the leg.

Introduction

The spring-mass model is a well-accepted construct used to characterize oscillations of the center of mass (CoM) during trotting, running, and hopping (Blickhan 1989; McMahon and Cheng 1990; Farley et al. 1993; Blickhan and Full 1993). By abstracting these "bouncing" gaits to a pogo-stick acting between the CoM and the ground, the spring-mass model imagines a single virtual leg that acts as a linear spring between the CoM and the substrate. Vertical oscillations are coupled with forward progression such that the virtual-leg rotates over the foot as it compresses and re-extends, hence, spring-loaded inverted pendulum (SLIP) is used interchangeably with spring-mass model. It is important to recognize that the spring-mass model or SLIP is a construct of a point-mass model that is energetically conservative and does not include the geometry, built-in springs, actuators, and dampers of actual physical legs.

The stiffness of the leg in a simple spring-mass model often has been estimated as the virtual-leg spring constant k_{leg} (McMahon and Cheng 1990) and this metric has been compared quantitatively to spring constants from SLIP-based simulations of

bipedal running (Blum et al. 2009). k_{leg} is the spring-constant of an energy-conservative virtual-leg spring with symmetry about mid-stance. Equation (1) gives the formula for k_{leg}, the ratio of maximum vertical force F_{max} to the estimated maximal deflection of the leg, ΔL:

$$k_{leg} = F_{max} / \Delta L \quad (1)$$

ΔL is estimated from initial leg length L_0, maximum vertical deflection of the CoM Δy, and the initial angle θ of the virtual leg with respect to vertical:

$$\Delta L = \Delta y + L_0(1 - \cos\theta) \quad (2)$$

In Equation (3), θ is in turn estimated from (i) initial length of the leg L_0 in the first instance of stance, (ii) duration of stance t_c, and (iii) average forward velocity during stance u.

$$\theta = \sin^{-1}\left(\frac{ut_c}{2L_0}\right) \quad (3)$$

The virtual-leg construct yielding k_{leg} has fueled key comparative studies of legged locomotion of arthropods and vertebrates spanning four to six orders of magnitude in body mass (Blickhan and Full 1993; Farley et al. 1993). k_{leg} has long been recognized to scale as the two-third power of body mass (Farley et al. 1993) or, equivalently, spring constant is independent of body mass when normalized by body mass and leg-length (Blickhan and Full 1993). These empirical results agree remarkably well with the predictions of dynamic similarity (Alexander and Jayes 1983) that maximum force should scale in direct proportion with body mass and that the leg should deflect by a constant proportion of leg-length, which in turn scales as body mass to the one-third power when animals trot, hop, or run at equal dimensionless speeds. Hence, two-third scaling of k_{leg} should be expected from Equation (1):

$$k_{leg} = F_{max} / \Delta L \propto m^1 / m^{1/3} = m^{2/3} \quad (4)$$

Empirical scaling relationships for F_{max} and ΔL deviate slightly yet reinforce the predicted two-third scaling of k_{leg} with body mass (Farley et al. 1993):

$$m^{0.67} = \frac{m^{0.97}}{m^{0.30}} \quad (5)$$

The two-third scaling of k_{leg} should not be considered an independent result because ΔL is estimated from initial leg-length, L_0 (Equations (2) and (3)). Given the similar exponents of $L_0 \propto m^{0.34}$ and $\Delta L \propto m^{0.30}$, ΔL is only influenced subtly by the scaling of the other terms in Equations (2) and (3). Empirical scaling exponents of these parameters are provided by Farley et al. (1993):

$$\Delta y \propto m^{0.36} \quad (6)$$

$$u \propto m^{0.12} \quad (7)$$

$$\theta \propto m^{-0.034} \quad (8)$$

$$t_c \propto m^{0.19} \quad (9)$$

Scaling of vertical deflection of the CoM ΔL was calculated in Equation (6) from the scaling of maximum vertical force $F_{max} \propto m^{0.97}$ and that of the vertical spring constant $k_{vert} \propto m^{0.61}$. The scaling exponent of ΔL will increase with that of θ according to Equation (2) such that a greater angle to the vertical yields a greater deflection of the virtual leg. The scaling exponent of θ will, in turn, increase with those of u and t_c, but will decrease with the exponent of L_0, according to Equation (3). In sum, the scaling of k_{leg} as mass to the two-third power is primarily a consequence of the direct proportionality of force with mass and the isometric scaling of leg-length as mass to the one-third power.

The k_{leg} metric has been widely used since its introduction (McMahon and Cheng 1990), in large part because it was the first method for quantifying the spring constant of the leg and because it can be calculated from force-plate data and two additional measurements: initial length of the leg L_0, and initial forward velocity u. However, the k_{leg} construct has several shortcomings: (i) k_{leg} is determined from a single measurement of force and an estimated deflection of the leg, instead of being determined from the dynamics of the physical legs throughout the stance and (ii) the assumption of symmetry is typically violated as asymmetrical ground reaction force (GRF; Table 1) is the norm during bouncing gaits (e.g., Lee et al. 2004; Cavagna 2006; McGowan et al. 2012; Andrada et al. 2013; Maykranz and Seyfarth 2014).

In contrast, we consider the spring constant of the physical leg during the non-conservative, asymmetrical dynamics that are measured experimentally as time-varying force and deflection throughout each instance of stance. The physical leg is modeled as a radial strut extending from the hip to the ground, and the radial-leg's spring constant k_{rad} (Table 1) is determined from the radial shortening and lengthening of the leg and the force in line with the radial axis of the leg. k_{rad} is determined iteratively based upon a serial actuator-spring model that minimizes the total mechanical work of the actuator while reproducing the experimentally measured force-deflection dynamics of the leg (Lee et al. 2008). Hence, this metric is distinct in (i) allowing for non-conservative mechanics, (ii) analyzing every instance of stance, (iii) being

Table 1 Notation

Symbol	Unit	Definition
h	m	Height of the hip during standing
g	ms^{-2}	Acceleration of gravity on Earth
$\overline{v}$	ms^{-1}	Mean forward velocity of the trunk during stance
$\sqrt{Fr}$		Square-root of the Froude number (Equation (11))
GRF	N	Ground reaction force—the resultant force exerted by the ground on the foot (trotters and runners) or feet (hoppers) during stance
F_n	N	Normal component of GRF
F_s	N	Shear component of GRF
F_{rad}	N	Component of GRF in-line with the radial leg
$\overline{F}_{rad}$	N	Mean of F_{rad} during stance
j_n	N-s	Time-integral of F_n during stance
j_s	N-s	Time-integral of F_s during stance
$\theta_{impulse}$	deg	Mean angle of the GRF impulse during stance (Equation (10))
L_{rad}	m	Length of the radial leg in each instance
$\overline{L}_{rad}$	m	Mean of L_{rad} during stance
V_{rad}	ms^{-1}	Time-derivative of L_{rad}
V_{act}	ms^{-1}	Time-derivative of the serial actuator's length
$\|W\|_{rad}$	J	Total work magnitude of the radial leg (Equation (12))
$\|W\|_{act}$	J	Total work magnitude of the actuator in the radial leg (Equation (13))
AR_{rad}		Actuation ratio of the radial leg (Equation (14))
k_{rad}	Nm^{-1}	Radial-leg spring constant yielding minimum $\|W\|_{act}$ and AR_{rad}

determined by minimization of actuator work, and (iv) analyzing the physical leg instead of a virtual leg originating at the CoM.

Methods

Subjects and experimental procedures: kangaroo rats and wallabies

Three tammar wallabies (*Macropus eugenii*) and three desert kangaroo rats (*Dipodomys deserti*) hopped bipedally along level runways while GRF and CoM trajectory were recorded. Table 2 provides body mass and leg-length for both species. All testing protocols were approved by the Harvard University (wallabies) or University of Idaho (kangaroo rats) Institutional Animal Care and Use Committees (IACUC). GRF of a pair of hind limbs was recorded with force plates at 1000 Hz (for wallabies: Kistler type 9286AA, Kistler Instrument Corp., Novi, MI, USA; for kangaroo rats: AMTI HE6X6, Advanced Mechanical Technologies Inc., Watertown, MA, USA). Trials were filmed in the sagittal plane with digital high-speed video cameras (125 Hz for the wallabies and 200 Hz for the kangaroo rats). White paint was used to mark the joints of the hind limbs, as shown in Fig. 1. Markers were tracked and digitized. The four trials nearest to steady-speed hopping were selected from each subject.

Subjects and experimental procedures: dogs and goats

Level trotting was recorded from three adult dogs (*Canis lupus familiaris*) and three adult goats (*Capra hircus*) on an indoor runway (10 m long) with a hard rubber surface. Table 2 provides body mass and leg-length for both species. A pair of rectangular force-platforms (AMTI BP400600HF, Advanced Mechanical Technologies Inc., Watertown, MA, USA) were embedded flush with the runway and oriented end-to-end with long axes parallel to the runway. All testing protocols were approved by Harvard University's IACUC committee. GRFs of the forelimbs and hind limbs were sampled at 2400 Hz for 5 s and these data were saved using a National Instruments DAQCard™ 6036E and LabView™ 7.1 (National Instruments, Austin, TX, USA). A Qualisys™ 3-D infrared system (3 ProReflex™ MCUs) and Qualisys Track Manager™ 1.6 software (Qualisys North America, Inc., Highland Park, IL, USA) were used for capturing motion. Retroreflective polystyrene hemispheres were used to mark the forelimb and hind limb joints, lateral hooves/paws, iliac crests, and the dorsal spine mid-way

Table 2 Body mass and basic parameters ± SD[a]

Species	m (kg)	$\overline{L}_{rad}$ (m)	$\sqrt{Fr}$	$\theta_{impulse}$ (deg)
Kangaroo rat—*Dipodomys deserti*	0.107 ± 0.014	0.054 ± 0.002	2.45 ± 0.36	0.21 ± 0.69
Tammar wallaby—*Macropus eugenii*	6.42 ± 0.48	0.284 ± 0.015	2.48 ± 0.74	2.33 ± 4.11
Dog—*Canis lupus familiaris*	23.5 ± 0.8	0.529 ± 0.035	1.19 ± 0.11	0.68 ± 1.16
Goat—*Capra aegagus hircus*	24.7 ± 2.3	0.479 ± 0.025	1.14 ± 0.13	−0.59 ± 3.08
Human—*Homo sapiens*	69.1 ± 7.1	0.794 ± 0.027	0.89 ± 0.08	−1.89 ± 2.60

[a]$\overline{L}_{rad}$ is the mean hind limb length during stance in bipeds, whereas $\overline{L}_{rad}$ is an average of mean forelimb and hind limb lengths in quadrupeds. For quadrupeds, the mean impulse angle $\theta_{impulse}$ is a weighted average of the forelimb and hind limb (60:40) to account for greater impulse of the forelimb.

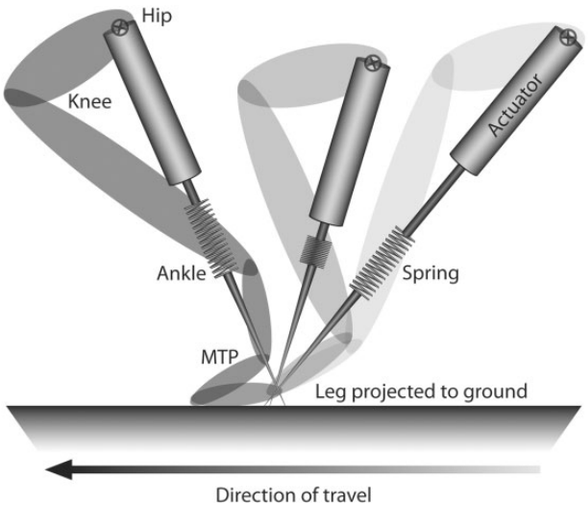

Fig. 1 Schematic of early, mid-stance, and late-stance phases illustrated by the hind limb of a wallaby. The radial-leg is defined as a line between the proximal joint (hip or scapulohumeral joint) and the foot (for quadrupeds) or projecting to the ground through the MTP (hoppers) or the ankle (humans). The serial actuator-spring model matches the force and deflection of the radial-leg throughout stance. The actuator is depicted as a piston and the in-series spring is depicted as a coil.

between the limb girdles. The 3-D positions of these markers were tracked at 240 Hz. The four trials nearest to steady-speed trotting were selected from each subject.

Subjects and experimental procedures: humans

Three adult human subjects (Table 2) ran at their preferred speed on a track with a pair of recessed Kistler types 9281B and 9281CA force-platforms (Kistler Instrument Corp., Novi, MI, USA). GRFs from individual legs were sampled at 1000 Hz using Vicon Nexus software. Informed consent was obtained prior to participation, as approved by the Internal Review Board at the University of Nevada, Las Vegas. Kinematic data were acquired using a 12-camera system (Vicon MX T40-S; 200 Hz; Vicon Inc., Los Angeles, USA), and 35-point spatial model (Vicon Plug-in Gait Fullbody). Filtering and interpolation of motion-capture data included a fourth order (zero lag) Butterworth lowpass filter (15 Hz) and cubic (third order) spline. The four trials nearest to steady-speed running were selected from each subject.

Kinetic and kinematic parameters

The GRF normal to the force platform's surface, F_n, and the component of shear force in the direction of travel, F_s, were used in a planar kinetic analysis (see Table 1 for parameter definitions). GRF directed toward the animal and forward in the direction of travel are considered positive. Normal impulse j_n and shear impulse j_s were determined by numerical integration of F_n and F_s over the contact period t_c. The resultant angle $\theta_{impulse}$ of j_n and j_s, defined with respect to normal, is given by

$$\theta_{impulse} = \tan^{-1}(j_s/j_n). \quad (10)$$

Positive angles indicate propulsion and negative ones indicate braking.

Kinematic analysis was restricted to the sagittal plane. Mean velocity in the direction of travel $\overline{v}$ was determined from the forward displacement of the trunk marker during the contact period and normalized as the square root of the Froude number,

$$\sqrt{Fr} = \overline{v}/\sqrt{gh}, \quad (11)$$

where g is the acceleration of gravity and h is the height of the hip when the animal is standing.

The length of the radial-leg L_{rad} is determined as the distance from the proximal joint (i.e., hip or scapulohumeral) and the hoof or second phalanx of the lateral digit for goats and dogs, respectively, in each instance of stance. To account for the long feet of bipeds, the radial-leg was projected from the hip joint through the metatarsophalangeal (MTP) joint of kangaroo rats and wallabies or through the ankle of humans to the ground. The component of force in-line with the radial leg F_{rad} is determined by

resolving the GRF vector into the radial axis of the leg in each instance of stance.

Serial actuator-spring model

In this report, the dynamics of the radial-leg(s) are determined in five different mammalian species during trotting, hopping, or running. A Hookean spring in-series with an actuator represents the action of all of the muscle-tendon systems about multiple joints (Fig. 1). The serial actuator-spring model for the radial-leg analyzes force F_{rad} and deflection (i.e., changes in L_{rad}) in every instance of stance. This model is used to determine the spring constant of the radial-leg and the fraction of work required from the in-series actuator of the radial-leg. The total (positive plus absolute value of negative) of work done by the radial-leg $|W|_{rad}$ and the total work done by its in-series actuator $|W|_{act}$ are determined from F_{rad} and the velocities of the radial-leg V_{rad} and its actuator V_{act}, respectively:

$$|W|_{rad} = \int |F_{rad} \times V_{rad}| dt \quad (12)$$

and

$$|W|_{act} = \int |F_{rad} \times V_{act}| dt. \quad (13)$$

$|W|_{act}$ is expressed as a fraction of $|W|_{rad}$ to yield a dimensionless actuation ratio AR_{rad}—a quantity between zero (completely Hookean) and unity (completely actuated). The spring constant determined by the model is the one which minimizes $|W|_{act}$ and consequently actuation ratio:

$$AR_{rad} = |W|_{act}/|W|_{rad}. \quad (14)$$

The radial-leg spring constant k_{rad} was determined iteratively by minimizing AR_{rad}. Using the least-squares regression of F_{rad} on L_{rad} as an initial estimate of k_{rad}, a range of $\pm 10^5$ spring constants was tried at intervals of $1\,Nm^{-1}$ (Lee et al. 2008).

Statistical analysis

In order to determine the relationships of k_{rad}, $\overline{F}_{rad}$, and $|W|_{rad}$ with body mass, these four parameters were first log-transformed, then tested in a least-squares model. $\sqrt{Fr}$ and $\theta_{impulse}$ were initially included as independent variables and removed if they were found to be non-significant ($P > 0.05$). The discrete variable *Species* was included as an independent variable to test whether it replaced the significance of body mass. If body mass became non-significant ($P > 0.05$), it was removed from the model and the allometric analysis was discarded in favor of interspecific comparisons using Tukey's Honest Significant Difference (HSD) test. Comparisons between dogs and goats of similar size were also carried out using a least-squares model and Tukey's HSD test without body mass as an independent variable. Parameter values in Tables 2 and 3 are simple means and standard deviations (SDs) for each species.

Results

Scaling of radial-leg spring constant k_{rad}

The radial-leg spring constant k_{rad} was determined by the serial actuator-spring model for kangaroo rats (0.107 kg) and wallabies (6.42 kg); two mammalian trotters: dogs (23.5 kg) and goats (24.7 kg); and humans running bipedally (69.1 kg) (Table 2). k_{rad} scales with an exponent of 0.70 when all five species are included ($P < 0.0001$; $R^2 = 0.98$; dashed line in Fig. 2A). There was no significant effect of dimensionless speed $\sqrt{Fr}$ or impulse-angle $\theta_{impulse}$ on k_{rad}. Goats are outliers in this allometric relationship, having a k_{rad} of $13.8\,kNm^{-1}$ that is nearly twice the k_{rad} of $7.5\,kNm^{-1}$ found in dogs. It is clear from Fig. 2A that the k_{rad} of goats falls substantially above the allometric curve determined for the five mammals included in this study. When goats are excluded and the allometric relationship of k_{rad} is recalculated with the four remaining species, a scaling exponent of 0.68 ± 0.02 is found ($P < 0.0001$;

Table 3 Radial-leg parameters ± SD[a]

Species	k_{rad} (kNm^{-1})	$\overline{F}_{rad}$ (kN)	AR_{rad}	$\lvert W\rvert_{rad}$ (J)
Kangaroo rat—*Dipodomys deserti*	0.206 ± 0.039	0.0026 ± 0.0004	0.42 ± 0.15	0.146 ± 0.031
Tammar wallaby—*Macropus eugenii*	3.40 ± 0.50	0.161 ± 0.023	0.39 ± 0.11	30.0 ± 7.5
Dog—*Canis lupus familiaris*	7.51 ± 1.33	0.315 ± 0.038	0.32 ± 0.06	40.7 ± 9.6
Goat—*Capra aegagus hircus*	13.81 ± 3.10	0.349 ± 0.031	0.37 ± 0.09	23.8 ± 5.4
Human—*Homo sapiens*	17.98 ± 3.98	0.941 ± 0.072	0.51 ± 0.13	222.5 ± 43.9

[a]Hind-limb values are shown for bipeds. For quadrupeds, k_{rad}, $\overline{F}_{rad}$, and $|W|_{rad}$ are sums of forelimb and hind-limb values and AR_{rad} is a weighted-average according to the fore-hind distribution of $|W|_{rad}$.

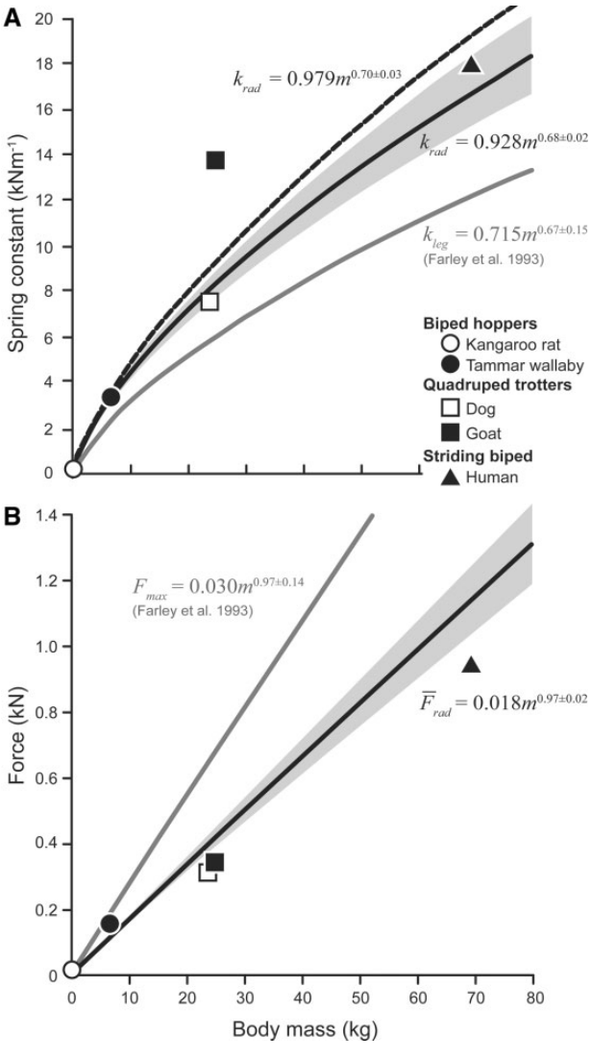

Fig. 2 Allometric relationship of the radial leg's spring-constant, k_{rad} **(A)** and mean radial-leg force $\overline{F}_{rad}$ **(B)** versus body mass in five mammals. Each plotted point is the mean of three subjects with four trotting/hopping/running steps each. Species and gait are identified by symbols in the key. In **(A)**, the power function for radial-leg spring constant k_{rad} is shown for all five species (dashed line; $R^2 = 0.98$) and with the goat excluded (solid line with shaded region showing 95% confidence interval of the exponent; $R^2 = 0.99$). The power function for the virtual-leg spring constant k_{leg} (gray line; Farley et al. 1993; $R^2 = 0.96$) is provided for comparison. In B, the power function for mean force of the radial-leg spring $\overline{F}_{rad}$ is shown (solid line with shaded region showing 95% confidence interval of the exponent; $R^2 = 1.0$) alongside the power function for peak leg force F_{max} (gray line; Farley et al. 1993; $R^2 = 0.97$).

$R^2 = 0.99$; black line in Fig. 2A). The k_{rad} for goats falls well above the 95% confidence interval of this power curve, whereas the other four mammals are contained within the 95% confidence intervals (shaded region of Fig. 2A). When goats are excluded, the scaling exponent for k_{rad} is not significantly different from two-third ($P < 0.05$).

The allometric scaling of the virtual-leg spring k_{leg} (Farley et al. 1993) is shown as a gray line in Fig. 2A for comparison with k_{rad}. Both these leg-spring constants scale with exponents that are not significantly different from two-third. Nonetheless, the allometric equation for k_{rad} shows a greater scaling coefficient of 0.928–0.979 versus 0.715 for k_{leg}; hence, the radial-leg's spring is stiffer than the virtual leg's spring at any body mass. In fact, the allometric curve for k_{leg} falls well outside of the 95% confidence limits of the allometric curve for k_{rad} (Fig. 2A).

Scaling of actuation ratio of the radial-leg AR_{rad}

The serial actuator-spring model selects a spring constant by minimizing the actuator work. Expressed as AR_{rad} (Equation (14)), the ratio of total work done by the actuator to total work done by the radial-leg, including work of both the actuator and spring, averaged between 0.32 and 0.42 for dogs, goats, wallabies, and kangaroo rats, in ascending order, but averaged 0.51 for human runners (Table 3). AR_{rad} was found to depend upon species to the exclusion of body mass, so Tukey's HSD was used to compare among species. Human runners have a significantly greater AR_{rad} than dogs or goats ($P < 0.05$) but other pair-wise comparisons are non-significant.

Scaling of mean force of the radial-leg $\overline{F}_{rad}$

The mean force in line with the leg $\overline{F}_{rad}$ scaled with an exponent of 0.97 ± 0.02 ($P < 0.0001$) when accounting for the significant effect of $\sqrt{Fr}$ ($P < 0.0001$; $R^2 = 0.99$) (Fig. 2B; Table 3). This multiple regression model accounts for the relatively slower speeds of dogs, goats, and humans compared with kangaroo rats and wallabies (Table 2). Although numerically close to unity, the scaling exponent of 0.97 is significantly different from direct proportionality of $\overline{F}_{rad}$ to body-mass ($P = 0.005$). There was no significant effect of impulse-angle $\theta_{impulse}$ on $\overline{F}_{rad}$.

Scaling of total work of the radial-leg $|W|_{rad}$

Total work of the radial-leg $|W|_{rad}$ scaled with an exponent of 1.23 ± 0.08 ($P < 0.0001$) and a coefficient of 1.25 when accounting for the significant effect of $\sqrt{Fr}$ ($P < 0.0001$; $R^2 = 0.97$) (Table 3). The scaling exponent of 1.23 is significantly different from the four-third scaling exponent ($P = 0.005$) predicted by dynamic similarity on the basis of direct proportionality of force and one-third scaling of leg deflection with mass. There was no significant effect of impulse-angle $\theta_{impulse}$ on $\overline{F}_{rad}$.

Comparison of goats and dogs

Given the nearly equal size of the dogs and goats included in this study (Table 2), a separate statistical analysis was used to make direct comparisons of the forelimbs and the hind limbs of these two quadrupeds. Hence, the independent variable body mass was replaced by the discrete variable *Species* (i.e., goat or dog) in this least-squares model. The mean force in line with the radial foreleg was influenced by dimensionless speed $\sqrt{Fr}$, while the moment-arm about the metacarpophalangeal (MCP) joint was influenced by both $\sqrt{Fr}$ and θ_{impulse} of the forelimb. There was no significant effect of $\sqrt{Fr}$ or θ_{impulse} on any of the radial hind-leg parameters, hence, the statistical model for the radial foreleg included $\sqrt{Fr}$ and θ_{impulse} plus the discrete variable *Species* as independent variables, whereas the statistical model for the radial hind-leg included only the discrete variable *Species*.

According to the serial actuator-spring model, k_{rad} is significantly greater in goats than in dogs ($P<0.0001$), indicating that the radial hind-legs of goats are 73% stiffer, and their radial forelegs are 145% stiffer than those of dogs (Fig. 3A,B). There is no effect of $\sqrt{Fr}$ on k_{rad} of the hind limb ($P=0.26$) or forelimb ($P=0.37$). There is no significant difference between goats and dogs in mean force $\overline{F}_{\text{rad}}$ of the radial hind-leg ($P=0.22$) or foreleg ($P=0.051$), nor is there a significant difference in actuation ratio AR_{rad} of the radial hind-leg

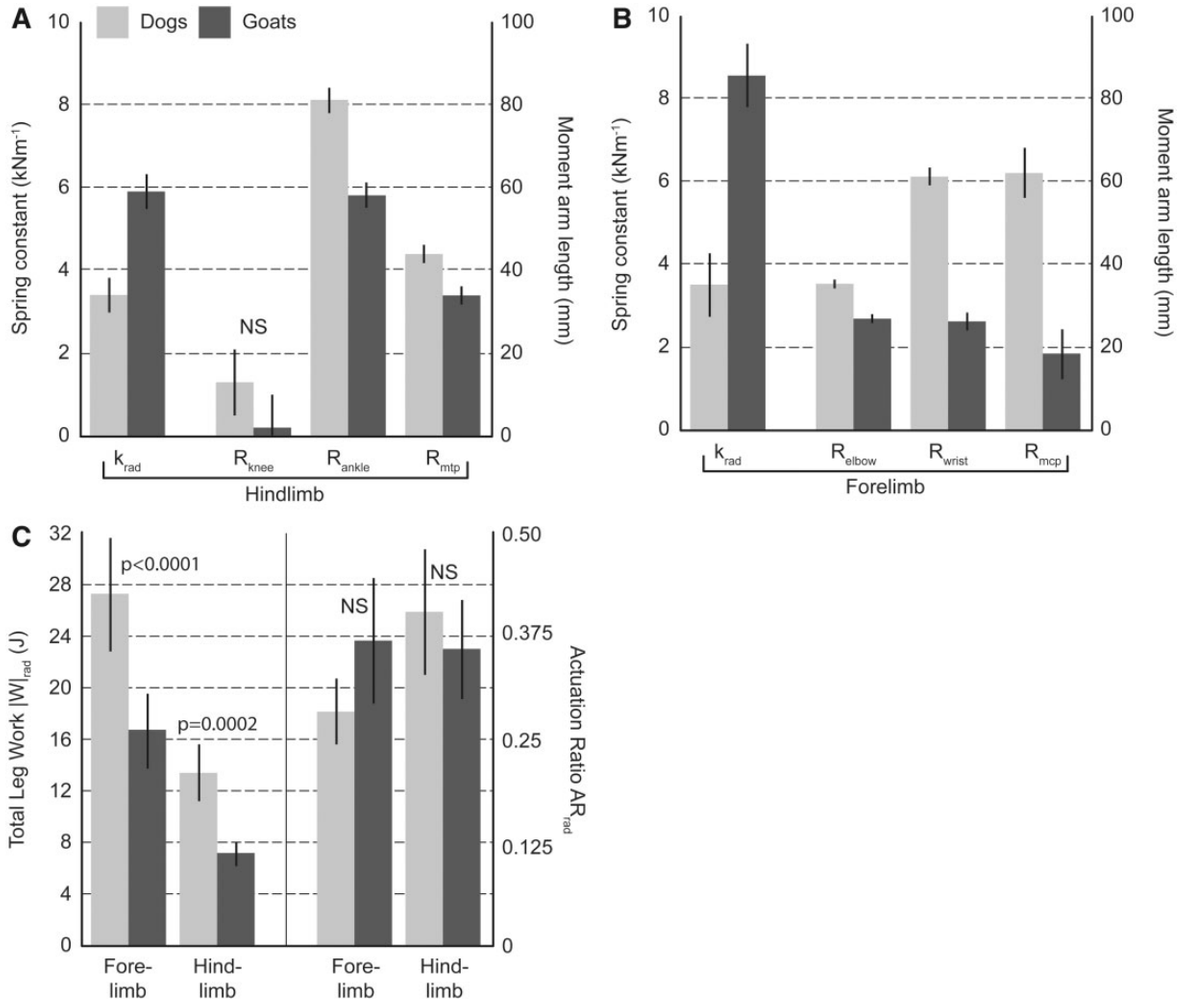

Fig. 3 Comparison of hind limbs **(A)** and forelimbs **(B)** of trotting dogs (light gray) and goats (dark gray) of similar body mass. Radial-leg spring constant k_{rad} is reported for the individual limb, whereas Fig. 2(A) shows the sum of the hind limb's and forelimb's spring constants. The mean moment arm R_{joint} of GRF about the three distal joints of the hind limb **(A)** and forelimb **(B)** are shown. **(C)** Total work $|W|_{\text{rad}}$ and actuation ratio AR_{rad} are shown for the radial hind-leg and radial foreleg of dogs (light gray) and goats (dark gray). Error bars are 95% confidence intervals. Goats and dogs are significantly different ($P<0.0001$) in all parameters that are not labeled with other values.

($P = 0.32$) or foreleg ($P = 0.15$) (Fig. 3C). Nonetheless, dogs show significantly greater $|W|_{rad}$ than goats in both the radial hind-leg and foreleg (Fig. 3C).

To address the mechanism of greater stiffness k_{rad} in the limbs of goats compared with dogs of similar size, the mean moment arm R_{joint} of the GRF is determined about each of the three joints between the foot and hip joint or foot and shoulder (scapulohumeral) joint. In the hind limb, R_{joint} of goats are significantly shorter than those of dogs about the MTP and ankle joints ($P < 0.0001$) but not about the knee ($P = 0.057$; Fig. 3A). Moment arms about the ankle and MTP of goats are, respectively, 72% and 77% those of dogs. In the forelimbs, R_{joint} of goats are significantly shorter about the MCP, wrist, and elbow joints ($P < 0.0001$; Fig. 3B) and are, respectively, 29, 43, and 77% those of dogs. There is no effect of $\sqrt{Fr}$ or $\theta_{impulse}$ on R_{joint} about hind limb and forelimb joints, except about the MCP, which decreases significantly with $\sqrt{Fr}$ ($P = 0.030$) and increases significantly with $\theta_{impulse}$ ($P = 0.028$).

Discussion

Scaling of radial-leg spring constant, k_{rad}

The scaling of spring constants as a two-third power of body mass is consistent with dynamic similarity (Alexander and Jayes 1983) as discussed by Farley et al. (1993). Dynamic similarity predicts that force scales as m^1 and, assuming that the change in leg-length is directly proportional to the initial length of the leg, deflection scales as $m^{1/3}$, hence, a spring-constant representing the ratio of force, and deflection would scale as $m^{2/3}$. This is true of k_{leg}, as it is largely determined by the ratio of peak leg-force to the initial leg-length, so it should not be expected to deviate much from two-third scaling. In contrast, k_{rad} is determined from the dynamic force-deflection pattern of the radial leg according to the serial actuator-spring model. The scaling result of k_{rad} is particularly compelling because it emerges from a physics-based model instead of depending upon a prescribed force-to-length ratio.

The geometry of the tendons provides a potential mechanism for two-third scaling of leg-spring constants. For example, the cross-sectional area of the *triceps surae* tendon is known to scale as the two-third power of body mass (Pollock and Shadwick 1994) across mammalian clades. Because limbs are complex multi-segmented systems, this explanation assumes that the average cross-sectional area of tendons and aponeuroses spanning multiple joints can be represented by the cross-sectional area of the *triceps surae* tendon. Because tendons are almost entirely collagen, their stiffness is primarily determined by the number of collagen fibrils in parallel, which is in turn proportional to the cross-sectional area of the tendon. A notable exception to two-third scaling among mammals is cross-sectional area of tendons within artiodactyla. A classic study found three-fourth scaling of tendons' cross-sectional area—a result consistent with elastic similarity among artiodactyls (McMahon 1975). Hence, an allometric study of artiodactyls, such as deer, antelope, cattle, goats, and sheep, might show that leg-spring constants increase as a three-fourth power of body mass because the tendons of artiodactyls scale according to elastic, rather than geometric, similarity. This is a potential explanation for the disparate k_{rad} of goats compared with the allometric relationship in the present study. A phylogenetic study applying the serial actuator-spring model would be required to support the hypothesis that tendons' cross-sectional area determines k_{rad} for artiodactyls as well as for mammals at large. The idea that the spring constants of legs may be determined by the thickness of collagen "ropes" spanning multiple joints is appealing in its simplicity. Nonetheless, detailed musculoskeletal modeling and simulation are necessary to substantiate the scaling of tendons' cross-sectional area as a mechanistic explanation for spring constants across species and size.

Despite the similarity of two-third scaling both in k_{rad} and k_{leg}, the scaling coefficient of k_{rad} is 30–37% greater than that of k_{leg} (Fig. 2A). Hence, the radial-leg spring constant k_{rad} is about one-third again as stiff as the virtual-leg spring-constant k_{leg} at any given body mass. A proximate explanation for this difference is that some of the deflection of the radial-leg is achieved by the actuator in the serial actuator-spring model, which represents the muscle in the leg. Because they are in series, the spring and the actuator are subjected to the same force. The serial actuator-spring model found that the work of the actuator was minimized with a stiffer spring than the virtual-leg model would predict. For example, a spring that is too compliant would deflect excessively, causing a greater compensatory deflection and consequently more work from the actuator. If built-in leg-springs (i.e., tendons) are too compliant and they are arranged in-series with their actuators (i.e., muscles), there is a risk that the compensatory deflection needed will exceed the shortening capacity of the muscle to "take up the slack." This would impose a limit on tendons' compliance because joints such as the ankle could hyper-flex or even collapse to a plantigrade posture due to unchecked

lengthening of the *triceps surae* tendon under load. Hence, the radial-leg spring constant k_{rad} is substantially greater than the virtual-leg spring constant k_{leg} and this greater stiffness reduces deflection of the built-in leg springs under a given load.

It might be possible to make tendons more compliant and thereby reduce the radial-leg spring constant to match the virtual-leg spring constant during level, steady-speed locomotion but this would neglect non-steady tasks such as locomotion on an incline or decline, propulsion or braking, jumping or landing, and falling. If the range of compensatory shortening of the muscle is a limiting factor, it is likely that tendons are made stiff enough to accommodate the forces expected during non-steady locomotion and locomotor perturbations. Using a serial actuator-spring model, a previous study found that spring constants of the radial hind-leg and the ankle joint were unchanged across level, uphill, and downhill locomotion of goats (Lee et al. 2008). This result is expected given that the *triceps surae* tendon is in-series with the ankle extensor muscles and there is no musculotendon system in-parallel that could modulate stiffness of the ankle appreciably. It should be emphasized that, regardless of the change in length of the extensor muscles, the stiffness about the ankle is limited by the stiffness of the *triceps surae* tendon because the actuator and spring are in-series. That is, the *triceps surae* tendon is held at its proximal end by a position-actuator while it interacts freely about the ankle through its insertion on the calcaneous. The stiffness about the ankle, in turn, limits the radial-leg spring constant k_{rad}.

In summary, the importance of non-steady locomotion, together with constraints on compensatory shortening of the muscle to "take up the slack," provides potential rationale for our present finding that k_{rad} is one-third again as stiff as k_{leg}. In addition to more accurately modeling biological systems, this insight may aid in the selection of appropriate spring constants for robotic prostheses and legged robots in which springs are used in series with actuators to achieve a range of locomotor tasks.

Comparison of goats and dogs

While dogs are excellent long-distance runners and terrain generalists, goats are specialists on rough, steep terrain. Given the disparity of these terrestrial niches, differences might be expected in the mechanics of the limbs of these two quadrupeds. While we do not have a sufficient survey for a phylogenetic analysis and, therefore, cannot distinguish goats as artiodactyls from goats as steep-terrain specialists, we can anticipate functional differences based on approximately two-fold greater spring constant k_{rad} observed in goats compared with dogs of similar size. Additionally, as mentioned in the previous section, anatomical evidence suggests the possibility that artiodactyls' legs have spring-constants that scale as mass to the three-fourth versus mass to the two-third for mammals in general.

Realizing that jumps and drops during ascent and descent of steep terrain entail greater leg-forces and that musculotendon springs are in-series, it is expected that radial-leg springs should be stiffer in goats. If this were not the case, stretching of the tendons could exceed the ability of the muscles to compensate by shortening and the joints could hyper-flex. The radial-leg spring constant is indeed 145% greater in the forelimb and 73% greater in the hind limb of goats compared with dogs (Fig. 3A,B). This disproportionate increase in stiffness of the forelimb is consistent with greater forces exerted on the forelimbs during vertical drops, which often are dramatic during evasion of predators. Goats diverged from other artiodactyls just 23 million years ago (Dong et al. 2013) and came to occupy an extreme alpine niche. Noting the absence of comparative data, if one assumes that artiodactyls have unusually stiff legs, this could be imagined as a locomotor pre-adaptation for steep terrain.

In an effort to understand the greater leg-spring constants of goats compared with dogs, we considered the moment arms of GRF about the distal limb-joints. This analysis showed that the moment arms of goats are significantly shorter about all joints but the knee. For a given leg-force, closer alignment of the GRF to these distal joints will reduce the moment about that joint, and thereby increase the resistance to angular deflection of that joint. The reduction of moment-arms appears to be a mechanism by which goats achieve greater radial-leg spring constants, yet this is not mutually exclusive of potential differences in the cross-sectional areas of the tendons.

Conclusions

We use a serial actuator-spring model to perform an allometric comparison across five species and show that radial-leg spring constant k_{rad} scales with the same two-third exponent predicted by dynamic similarity and as modeled by the virtual-leg spring-constant k_{leg} for trotting, hopping, and running mammals. This not only supports an effect of body-mass that holds across different modeling

approaches and agrees with dynamic similarity, but it also offers the first evidence from an independent model for two-third scaling that is derived from actual leg dynamics. Based on scaling coefficients, k_{rad} is one-third again as stiff as k_{leg} at any given body-mass, which may reflect a need for stiffer built-in springs (i.e., tendons) to sustain greater forces without excessive deflection during non-steady locomotion. Goats are significant outliers with radial-leg spring constants nearly two-fold greater than those of dogs of similar size, suggesting that artiodactyls have stiffer legs and/or goats are specialized for rough, steep terrain. Allometric analyses of artiodactyls are needed to explore these possible explanations. Additionally, comparative data from a size-range of rodents, macropods, and carnivores are needed to confirm two-third scaling of the spring constant of legs within clades and to detect any differences between trotting, hopping, and running gaits.

Acknowledgments

We thank Dayne Sullivan, Tudor Comanescu, Andrew Nordin, and Joshua Bailey for the help with the collection of data, and Pedro Ramirez for animal-care support.

Funding

This work was supported in part by Defense Advanced Research Projects Agency grant BIOD_0010_2003 [BAA #01-42]; from the National Institute of General Medical Sciences [P20GM103440]; from the National Institutes of Health and by BEACON under NSF Cooperative Agreement [DBI-0939454]; and by IDeA Networks of Biomedical Research Excellence [NIH grant nos. P20 RR016454 and P20 GM103408].

References

Alexander R, Jayes AS. 1983. A dynamic similarity hypothesis for the gaits of quadrupedal mammals. J Zool 201:135–52.

Andrada E, Nyakatura JA, Bergmann F, Blickhan R. 2013. Adjustments of global and local hind limb properties during terrestrial locomotion of the common quail (Coturnix coturnix). J Exp Biol 216:3906–16.

Blickhan R. 1989. The spring-mass model for running and hopping. J Biomech 22:1217–27.

Blickhan R, Full RJ. 1993. Similarity in multilegged locomotion: bouncing like a monopode. J Comp Physiol 173: 509–17.

Blum Y, Lipfert SW, Seyfarth A. 2009. Effective leg stiffness in running. J Biomech 42:2400–5.

Cavagna GA. 2006. The landing–take-off asymmetry in human running. J Exp Biol 209:4051–60.

Dong Y, Xie M, Jiang Y, Xiao N, Du X, Zhang W, Wang W. 2013. Sequencing and automated whole-genome optical mapping of the genome of a domestic goat (*Capra hircus*). Nat Biotechnol 31:135–41.

Farley CT, Glasheen J, McMahon TA. 1993. Running springs: speed and animal size. J Exp Biol 185:71–86.

Lee DV, Stakebake EF, Walter RM, Carrier DR. 2004. Effects of mass distribution on the mechanics of level trotting in dogs. J Exp Biol 207:1715–28.

Lee DV, McGuigan MP, Yoo EH, Biewener AA. 2008. Compliance, actuation, and work characteristics of the goat foreleg and hindleg during level, uphill, and downhill running. J App Physiol 104:130–41.

Maykranz D, Seyfarth A. 2014. Compliant ankle function results in landing-take off asymmetry in legged locomotion. J Theoret Biol 349:44–9.

McGowan CP, Grabowski AM, McDermott WJ, Herr HM, Kram R. 2012. Leg stiffness of sprinters using running-specific prostheses. J Royal Soc Interface 9:1975–82.

McMahon TA. 1975. Using body size to understand the structural design of animals: quadrupedal locomotion. J Appl Physiol 39:619–27.

McMahon TA, Cheng GC. 1990. The mechanics of running: how does stiffness couple with speed? J Biomech 23:65–78.

Pollock CM, Shadwick RE. 1994. Allometry of muscle, tendon, and elastic energy storage capacity in mammals. Am J Physiol Regul Integr Comp Physiol 266:R1022–31.